

SMALL-ANGLE NEUTRON SCATTERING ON MAGNETIC FLUIDS STABILIZED BY MONOCARBOXYL ACIDS

A.V. FEOKTYSTOV, L.A. BULAVIN¹, M.V. AVDEEV, L. VEKAS²,
V.M. GARAMUS³, R. WILLUMEIT³

UDC 538.97

©2009

Joint Institute for Nuclear Research
(Dubna, Russia),

¹Taras Shevchenko Kyiv National University
(Kyiv, Ukraine),

²Centre of Fundamental and Advanced Technical Research
(Timisoara, Romania),

³GKSS Research Center
(Geesthacht, Germany)

Using the method of variation of a contrast in the small-angle scattering of non-polarized thermal neutrons, we have investigated the magnetic liquid systems on the basis of water having steric stabilization. As magnetic nanoparticles, we used magnetite particles covered by lauric or myristic acid. Applying a new method of basic functions to the study of polydisperse superparamagnetic systems, we have got data on the structural features of magnetic fluids for the size range (1÷100) nm. We have found that the form of aggregates of magnetic particles depends on the type of a surfactant stabilizing the magnetic liquid system. It is shown that the samples treated by lauric acid have the best stabilization properties.

1. Introduction

Magnetic liquids are such liquid systems [1] that are formed by means of the introduction of magnetic nanoparticles in a certain liquid. To prevent the aggregation of nanoparticles due to the dipole-dipole interaction (especially in a magnetized state under the action of an external magnetic field), magnetic particles are usually covered by the stabilizing layer of a surface-active substance (SAS) [2]. In the case of nonpolar organic solvents, one layer of SAS adsorbed on the surface of magnetic particles efficiently hampers the aggregation of magnetic particles. In the case of polar magnetic fluids, it is necessary to form the second layer for the stronger stabilization [3, 4]. In this case, the first layer is created by means of the chemical adsorption of polar heads of SAS on the surface of magnetic particles. The second layer is a result of the physical sorption: the tails of molecules of the second stabilizing layer are directed to the tails of molecules of the first stabilizing layer. Thus, the polar heads of SAS are oriented outward, which allows one to retain

particles in polar carriers. Such a kind of stabilization by the formation of a double layer requires the existence of an excess of molecules of SAS in a solution. In this case, the exchange between molecules of the second stabilizing layer and free molecules in a solution is in equilibrium. We note that the magnetic liquid systems on the basis of water are promising for the synthesis of biocompatible magnetic systems with their further use in various medical branches such as magnetic hyperthermia in the treatment of cancer [5,6] and transport of drugs [7] or as a contrast medium in magnetic resonance imaging [6, 7].

Even in the absence of an external magnetic field, the main problem of the synthesis of aqueous magnetic liquids with steric stabilization is related to the formation of aggregates, which testifies to the absence of the full stabilization of nanoparticles in such liquid systems. It was shown earlier [4, 8, 9] that complex aggregates with various sizes can arise in magnetic aqueous systems. The bulk share of a magnetic material (magnetite) was not exceed 5% in such liquid systems. Recently, it was proposed to use short monocarboxyl acids [lauric acid (LA), $\text{CH}_3(\text{CH}_2)_{10}\text{COOH}$, and myristic acid (MA), $\text{CH}_3(\text{CH}_2)_{12}\text{COOH}$], which allows one to increase the content of magnetite to at least 10% [3].

The purpose of the present work is the study of a structure of new magnetic liquid systems with the help of the small-angle scattering of nonpolarized thermal neutrons (SANS) with the use of the contrast variation technique which is based on a partial replacement of hydrogen by deuterium in water which is the basis of a magnetic liquid system. Such a replacement significantly changes the neutron scattering which is determined by a difference of the densities of the

scattering lengths of components in the system under study. In the experiments with the help of SANS, the contrast variation was realized for nonmagnetized specimens (without magnetic field). Nanomagnetite dispersed in the studied magnetic liquid systems was characterized by a wide distribution function of sizes, which complicated the use of the classical contrast variation procedure in SANS [10]. In view of this, with the purpose to determine the structural peculiarities of liquid systems in the range (1÷100) nm, we choose a new approach of basic functions in the contrast variation method which was developed earlier to study the polydisperse multicomponent superparamagnetic systems [11]. The results of our neutron studies of a structure of magnetic liquid systems are compared with the data of electron microscopy [12].

2. Experimental Procedure

The magnetic liquid systems under study were synthesized at the Laboratory of magnetic liquids of the Centre of Fundamental and Advanced Technical Research of the Romanian Academy of Sciences (Timisora, Romania).

The bulk share of dispersed magnetite ϕ_m was 11% in the LA specimen and 13% in the MA specimen. Liquid systems possessed a good stability in the absence of an external magnetic field (at least for one year after the fabrication).

In order to perform the measurements of the small-angle scattering of neutrons with the use of the contrast variation method, the produced magnetic liquid systems were diluted by ten times by light (H_2O) and heavy water (D_2O) so that the bulk share of D_2O in the net specimen was varied from 0% to 90%.

The measurements were executed on the SANS-1 installation [13] at the steady-state reactor FRG-1 of the GKSS Research Center (Geesthacht, Germany). We determined the differential scattering cross-section per unit volume (scattering intensity), which is isotropic relative to the momentum transfer vector \vec{q} , as a function of the modulus of the momentum transfer vector $q = (4\pi/\lambda)\sin(\theta/2)$, where λ is the wavelength of a neutron, and θ is the scattering angle. The specimens were positioned in a quartz cuvette with a thickness of 1 mm (Hellma) and held at a temperature of 25 °C during the experiment. In this case, no magnetic field was applied. We obtained the scattering curves on the fixed neutron wavelength equal to 0.83 nm (the

monochromatization error $\Delta\lambda/\lambda = 10\%$) for the series of distances between a specimen and a detector from 0.7 to 9.7 m (the detector area was $55 \times 55 \text{ cm}^2$, and the spatial resolution was $0.7 \times 0.7 \text{ cm}^2$) in the interval of q from 0.06 nm^{-1} to 2.5 nm^{-1} . We used the standard procedure of the calibration of measurements by the intensity of the small-angle scattering of neutrons on water. As a buffer, we used the relevant solutions H_2O/D_2O with the corresponding content of D_2O .

As known [14], the contrast variation method in SANS is based on the registration of changes in the scattering on the system under a change in the contrast, namely, the difference between the mean densities of the scattering lengths of particles and a solvent. In the classical generalized approach for monodisperse nonmagnetic particles, the intensity of SANS is analyzed [11] in terms of basic functions (the q -dependent coefficients of the expansion of I over the contrast). For polydisperse magnetic particles in magnetic liquid systems, the scattering can be also treated in a similar way [11]:

$$I(q) = \tilde{I}_s(q) + \Delta\tilde{\rho}\tilde{I}_{cs}(q) + (\Delta\tilde{\rho})^2\tilde{I}_c(q), \quad (1)$$

where

$$\Delta\tilde{\rho} = \bar{\rho}_e - \rho_s \quad (2)$$

is the so-called modified contrast, namely, the difference between the effective mean density of the scattering lengths of particles $\bar{\rho}_e$ and the density of the scattering lengths of a liquid-carrier ρ_s ; $\tilde{I}_c(q)$, $\tilde{I}_s(q)$, $\tilde{I}_{cs}(q)$ are the modified basic functions which contain the information about the distributions of the nuclear and magnetic densities of the scattering lengths inside magnetic particles. The term $(\Delta\tilde{\rho})^2\tilde{I}_c(q)$ gives the main contribution to the scattering intensity at sufficiently large contrasts and corresponds to the averaged form of a particle:

$$\tilde{I}_c(q) = \int D_N(R)I_c(qR)dR, \quad (3)$$

where $D_N(R)$ – radius distribution function of particles; $I_c(qR)$ – Fourier transform of the scattering length density distribution of a particle (form-factor); $\tilde{I}_s(q) = I_N(q)|_{\Delta\tilde{\rho}=0} + I_M(q)$ – term which depends on the contrast and includes the residual nuclear scattering $I_N(q)$ at the effective match point and the contribution from the magnetic scattering $I_M(q)$ which is determined by the magnetic scattering length density of a particle. $I_{cs}(q)$ – cross term.

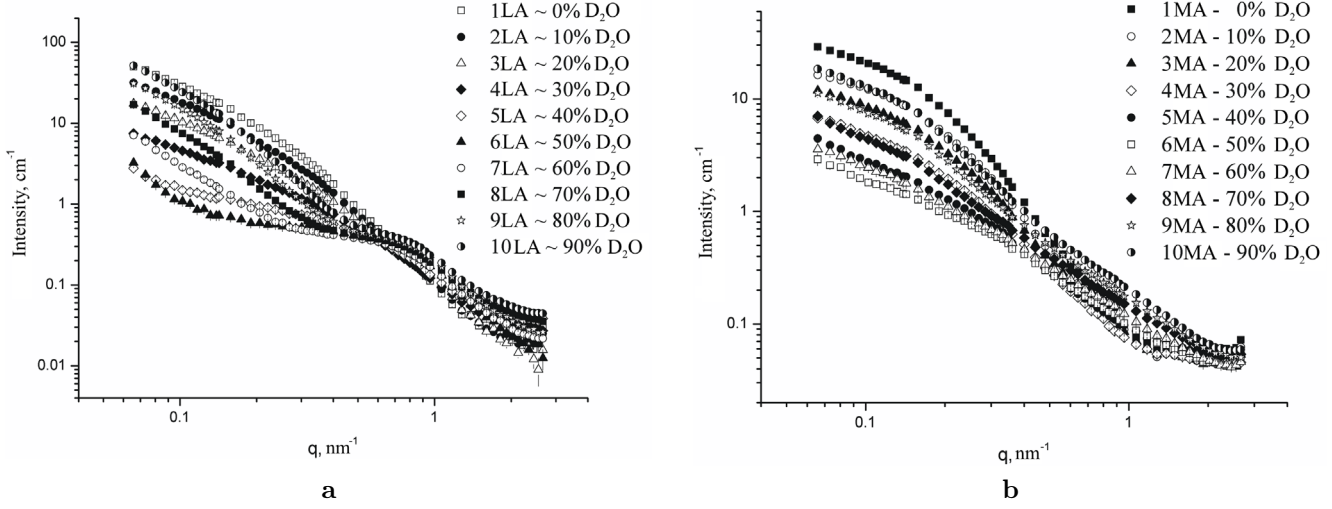


Fig. 1. Variation of the contrast in SANS on magnetic liquids with the double stabilization by lauric (LA) (a) and myristic acids (MA) (b). The bulk share of D_2O in % in a solvent is indicated. The bulk shares φ_m of dispersed magnetite in the specimens are $\sim 1.1\%$ (LA) and $\sim 1.3\%$ (MA)

3. Results of the Experiment and Their Discussion

The scattering curves obtained by us at various contents of D_2O are given in Fig. 1,*a* (LA) and Fig. 1,*b* (MA). It is worth noting that the densities of scattering lengths for SAS (approximately $0.10 \times 10^{10} \text{ cm}^{-2}$) and H_2O ($-0.56 \times 10^{10} \text{ cm}^{-2}$) are quite close. This means that the scattering in specimens fabricated on the basis of H_2O occurs mainly on magnetite ($6.90 \times 10^{10} \text{ cm}^{-2}$). In the cases close to D_2O ($6.34 \times 10^{10} \text{ cm}^{-2}$), the scattering on SAS significantly differs from the scattering on a solvent, which is reflected in the appearance of specific features of the scattering curves, as compared with the case of H_2O (Fig. 1). While analyzing the experimental data, we modeled spherical magnetite particles covered by a layer of SAS, but we failed to approximate the obtained experimental curves within the “core-shell” model for separate particles. In our opinion, this indicates a significant influence of the aggregation of particles on the scattering of neutrons, which strongly separates the magnetic liquid systems under study from those formed on the basis of nonpolar solvents with the addition of nanoparticles which are stabilized by one layer of SAS [15]. The scattering on aggregates makes it impossible to process the obtained curves by using the Guinier approximation [14]. In its turn, the standard procedure of variation of the contrast uses, as the first step, the analysis of the dependence of the neutron scattering intensity at the zero angle $I(0)$, which is determined

from the Guinier approximation, on the contrast. In particular, the effective match point in the case of polydisperse systems can be referred to the minimum of a parabolic dependence of $I(0)$ on the content of D_2O in the liquid base. Because of the effect of aggregation of magnetite nanoparticles here, we made an arbitrary choice of the effective match point for the determination of a modified contrast. Nevertheless, we can carry out a certain analysis which relates this choice with the internal structure of the liquid systems under study. In Fig. 2, we present the intensities of the small-angle scattering of neutrons on liquid systems depending on the content of D_2O for various values of q for two specimens. If the particles are homogeneous, then the positions of minima in such parabolic dependences must not vary, and then the positions of minima correspond to the mean density of the scattering length of particles. For inhomogeneous particles, the positions of minima on the mentioned dependence will shift with a change of q . The obtained positions of minima as functions of q are shown in Fig. 3. The important observation is that the position of the minimum for the MA specimen does not change in the interval of q from 0.06 to 0.3 nm^{-1} . Thus, we may conclude that the aggregates in the studied specimen can be considered as homogeneous with sizes more than 20 nm. The relevant effective match point, 51% D_2O , indicates that the mean density of the scattering lengths of aggregates is $2.93 \times 10^{10} \text{ cm}^{-2}$. At the same time, for the LA specimen, it is impossible to find such an interval of q , in which the match point

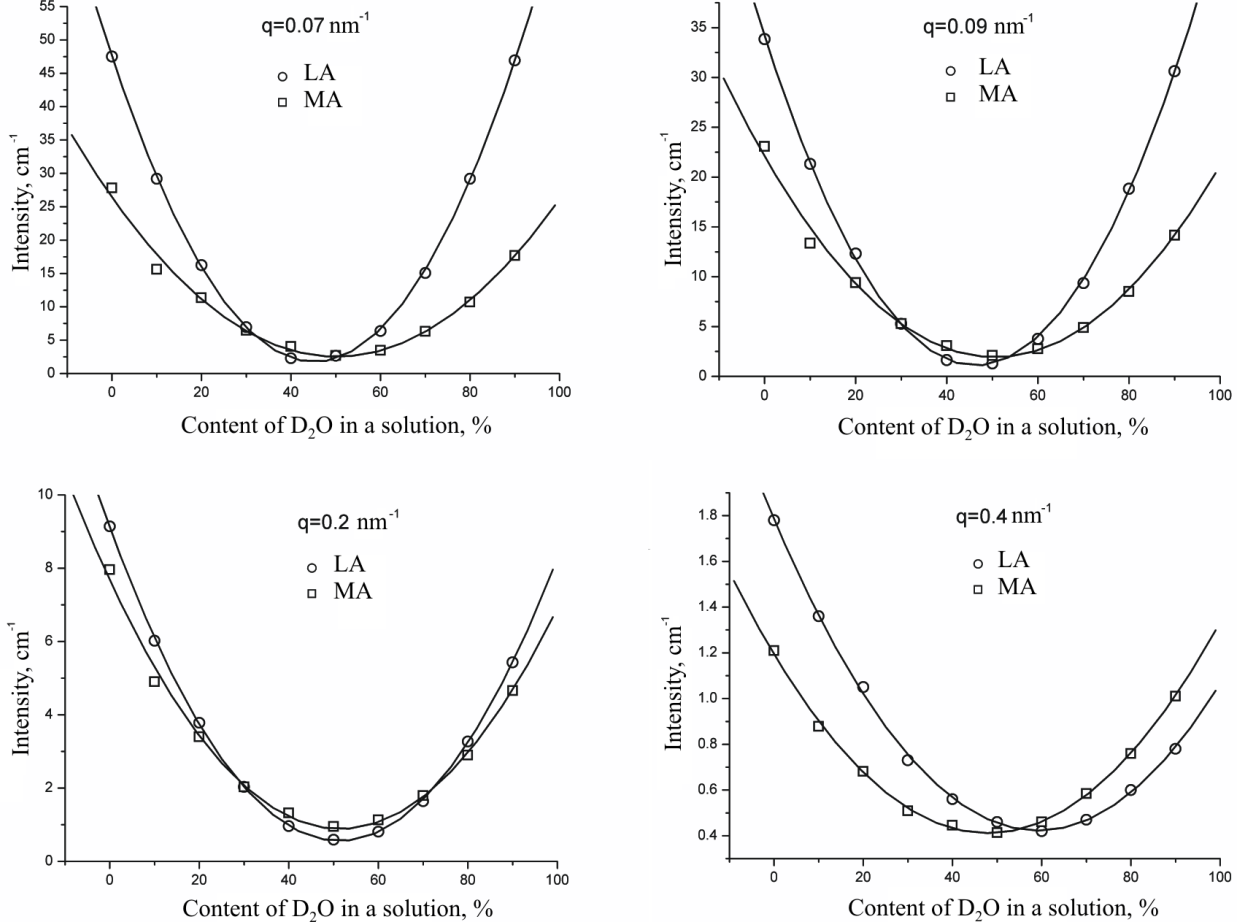


Fig. 2. Intensity of the small-angle scattering of neutrons on the magnetic liquid systems stabilized by LA and MA versus the content of D_2O in a solvent at various values of q

does not change. That is, in this case, we deal with sufficiently polydisperse aggregates, whose mean density of the scattering lengths significantly depends on the size of an aggregate.

In order to determine the modified contrast (2), we used the dependences of the scattering intensities on the content of D_2O at $q = 0.09 \text{ nm}^{-1}$. The determined positions of minima give the effective match points at 46.6% (the relevant density of the scattering lengths is $2.642 \times 10^{10} \text{ cm}^{-2}$) and 50.6% (the relevant density of the scattering lengths is $2.931 \times 10^{10} \text{ cm}^{-2}$) contents of D_2O for the LA and MA specimens, respectively. With the purpose to find the basic functions $\tilde{I}_c(q)$, $\tilde{I}_s(q)$, $\tilde{I}_{cs}(q)$ from the experimental data, we minimized the functional [16]

$$\chi^2 = \frac{1}{N-3} \times$$

$$\times \sum_k \frac{[I_k(q) - \tilde{I}_s(q) - \Delta\tilde{\rho}_k \tilde{I}_{cs}(q) - (\Delta\tilde{\rho}_k)^2 \tilde{I}_c(q)]^2}{\sigma_k^2(q)}, \quad (4)$$

where $I_k(q)$ and $\sigma_k(q)$ – the experimental scattering intensity and its error at the given q for each k -th modified contrast; and N – total number of curves obtained for different contrasts.

The obtained modified basic functions are given in Figs. 4–7. The check out of the developed procedure consists in the comparison of the function $\tilde{I}_s(q)$ obtained in such a way with the experimental curves registered at a content of D_2O which is close to the effective match point. As shown in Fig. 4, $\tilde{I}_s(q)$ repeats the scattering signal at the effective match point. At the same time, the function $\tilde{I}_{cs}(q)$ (Fig. 5) is significantly different from that for monodisperse particles, which indicates a large polydispersity of particles.

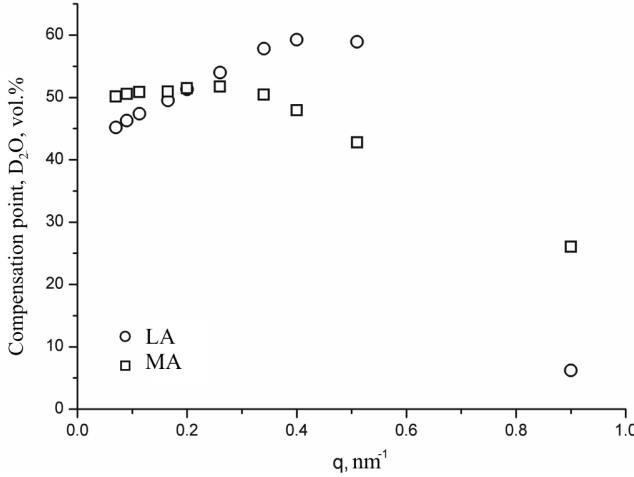


Fig. 3. Effective match point versus q for the magnetic liquid systems stabilized by LA (○) and MA (□)

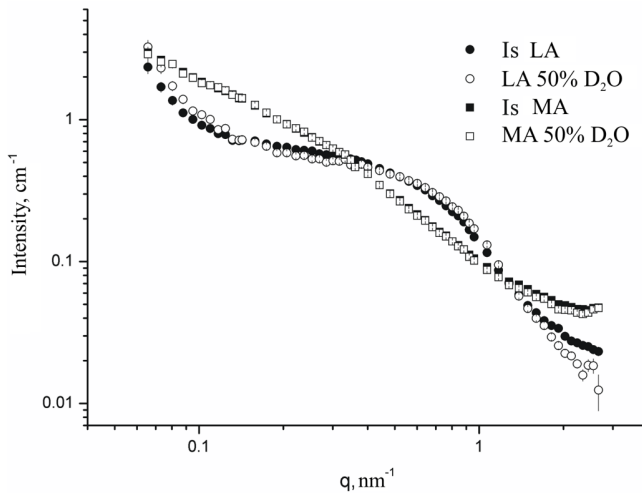


Fig. 4. Comparison of the experimentally obtained basic functions $\tilde{I}_s(q)$ for the magnetic liquid systems with the scattering curves at the 50-% content of D₂O in the liquid base which are close to the effective match points of the corresponding magnetic fluids

The most informative from all the modified basic functions is the function $\tilde{I}_c(q)$. The comparison of the functions $\tilde{I}_c(q)$ for the LA and MA specimens (Fig. 6) indicates that particles of the magnetic liquid LA system have larger sizes than particles of the magnetic liquid MA system. This is well confirmed by the inverse Fourier transformation (IFT) [17] of the function $\tilde{I}_c(q)$, whose result is the distance distribution function $p(r)$ which is shown in Fig. 7. For polydisperse systems, this function reflects the size distribution of particles. The largest

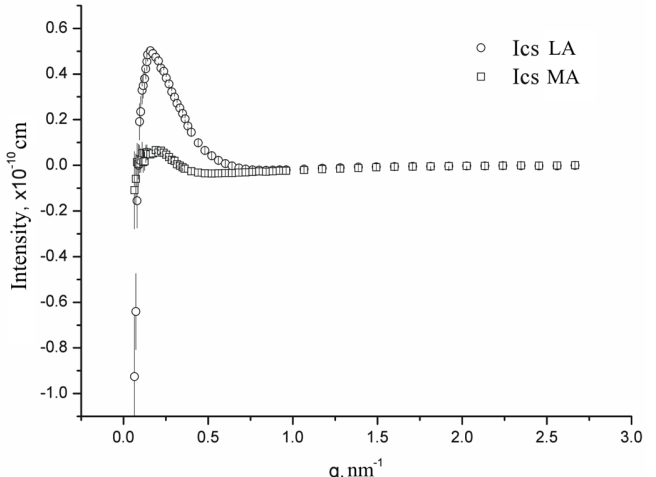


Fig. 5. Experimentally obtained function $\tilde{I}_{cs}(q)$ for the magnetic liquid systems stabilized by LA (○) and MA (□)

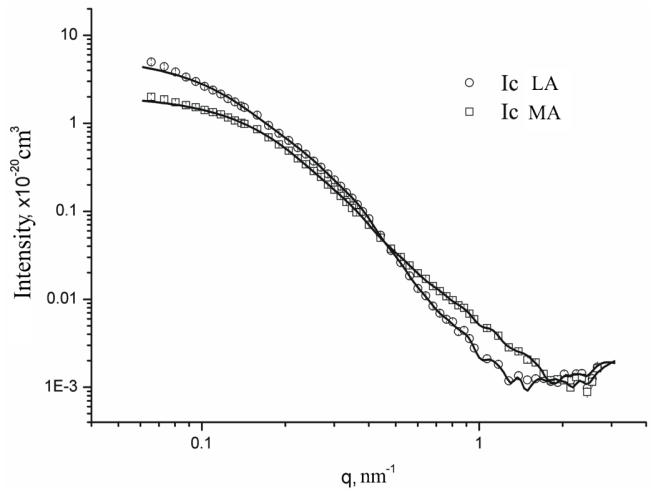


Fig. 6. Experimentally obtained basic functions $\tilde{I}_c(q)$ for each of the studied magnetic liquid systems. Lines show the approximations of the curves. The parameters of IFT: $R_g = (15.1 \pm 0.2)$ nm, $I(0) = (5.8 \pm 0.1) \times 10^{-20}$ cm³ for LA and $R_g = (10.7 \pm 0.1)$ nm, $I(0) = (2.1 \pm 0.1) \times 10^{-20}$ cm³ for MA

value, where $p(r)$ is nonzero, corresponds to the largest size of aggregates equal, respectively, to 49 and 33 nm for the LA and MA specimens and agrees completely with our conclusion presented above. The radius of gyration R_g calculated by us with the use of the function $p(r)$ equals (15.1 ± 0.2) nm for LA and (10.7 ± 0.1) nm for MA and is connected with the radius of gyration of particles R_c and their volume V_c by the formula $R_g^2 = \langle R_c^2 V_c^2 \rangle / \langle V_c^2 \rangle$, where the brackets mean the averaging over the radius distribution functions of particles

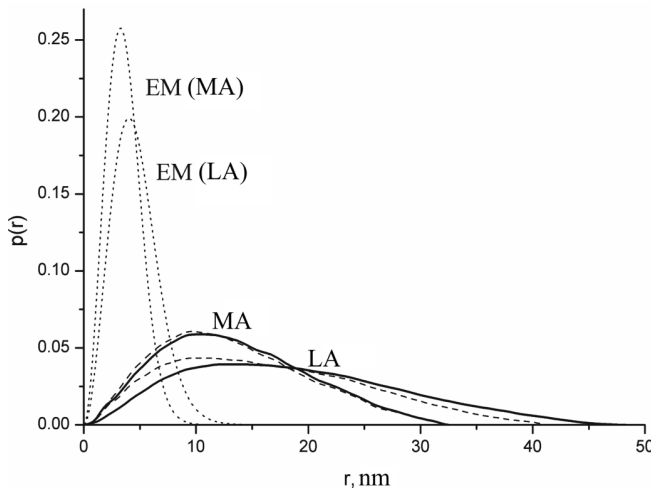


Fig. 7. Distance distribution functions of particles obtained from the basic functions $\tilde{I}_c(q)$ for the studied magnetic liquid systems (solid lines) which are compared with the distance distribution functions obtained from the curves with zero content of D_2O (dashed lines) and with the measurements executed with the help of electron microscopy of individual particles (dotted lines) – MA $D_0 = 6.08 \text{ nm}$, $S = 0.20$; LA: $D_0 = 7.42 \text{ nm}$, $S = 0.23$

$D_N(R)$. Under the assumption of a quasispherical form of aggregates, the relation $R_c^2 = (3/5)R^2$ yields the characteristic radii of particles $(\langle R^2 V_c^2 \rangle / \langle V_c^2 \rangle)^{1/2}$ which equal, respectively, (19.5 ± 0.3) and (13.8 ± 0.1) nm for the LA and MA specimens. In Fig. 7, the distance distribution functions obtained by us from $\tilde{I}_c(q)$ are compared with those determined by us from the scattering curves with the zero content of D_2O . We note that, in the last case, the small-angle scattering of neutrons is determined only by the scattering on magnetite. In addition, Fig. 7 presents the distance distribution functions calculated by us for separate magnetite nanoparticles in magnetic liquid systems. The calculations were based on data [12] of electron microscopy which gave the log-normal distribution function of the radii of particles,

$$D_N(R) = (1/2\pi)^{1/2} (SR)^{-1} \exp[-\ln^2(R/R_0)/2S^2], \quad (5)$$

with the parameters $R_0 = 3.7 \text{ nm}$, $S = 0.23$ (LA) and $R_0 = 3.0 \text{ nm}$, $S = 0.20$ (MA).

The analysis of Fig. 7 reveal the existence of the essential difference in the formation of aggregates in the case of the magnetic liquid systems under study. For the LA specimen, we notice a remarkable difference in the distance distribution functions obtained from the curves $\tilde{I}_c(q)$ and H_2O . As for the MA specimen, the distance distribution functions almost coincide for such curves.

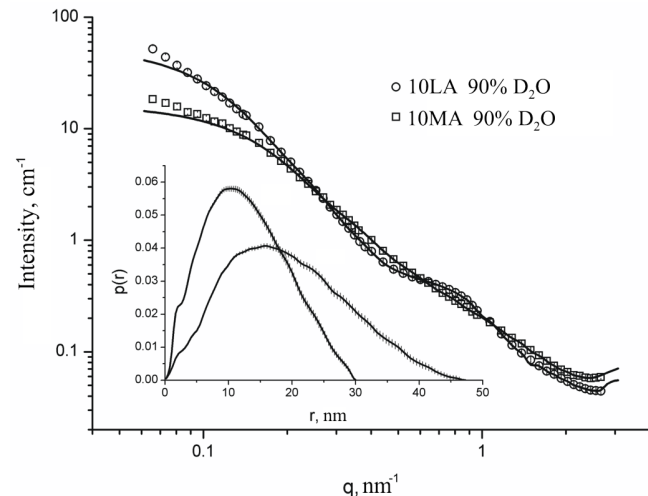


Fig. 8. Curves of the small-angle scattering of neutrons on the specimens with the 90-% content of D_2O in a solvent. Lines correspond to the approximation of curves. The inset shows the relevant distance distribution functions. The parameters of IFT: $R_g = (15.2 \pm 0.2) \text{ nm}$, $I(0) = (54.8 \pm 1.6) \text{ cm}^{-1}$ (LA) and $R_g = (10.2 \pm 0.1) \text{ nm}$, $I(0) = (16.3 \pm 0.3) \text{ cm}^{-1}$ (MA)

For the LA specimen, the difference of the maximum sizes for two distance distribution functions equal approximately to 3.5 nm can be referred to the effective thickness of the SAS layer near magnetite nanoparticles. The fact that separate particles which form aggregates have larger sizes and a greater polydispersity in the LA specimen (see the data of electron microscopy in Fig. 7) explains, in our opinion, a larger size and a greater polydispersity of aggregates in this specimen. As for the MA specimen, we consider that this case is characterized by a homogeneous agglomeration with a sufficiently small effective thickness of SAS around separate magnetite nanoparticles. With regard for both the mean density of the scattering lengths of aggregates in the MA specimen obtained by us from the analysis of the effective match point and the fact that the densities of the scattering lengths of SAS and the densities of possible voids in aggregates are close to zero, we can estimate the bulk share of magnetite ε_m as

$$\varepsilon_m \sim \bar{\rho}_e / \rho_m, \quad (6)$$

where $\bar{\rho}_e$ – mean density of the scattering lengths for an aggregate, and ρ_m – the density of the scattering lengths for magnetite. Our estimate of the bulk share of magnetite gives $\varepsilon_m = 0.44$. This means that the share of SAS in aggregates does not exceed 56%. By using the function $D_N(R)$ determined by electron microscopy for

separate particles of magnetite, we get that the largest effective thickness of SAS around magnetite which would agree with the determined content of SAS is bounded by a value of 1.3 nm. In order to get agreement with the fact that the distance distribution functions for magnetite and aggregates are identical, we should state the existence of an incomplete coverage of magnetite by molecules of SAS in the MA specimen. In other words, the particles in aggregates are nanomagnetite covered by a single incomplete layer of myristic acid. On the other hand, the magnetic liquid LA system can be considered as the closest to nonpolar organic magnetic liquids [15] with the “core-shell” structure of particles, where molecules of SAS cover completely the surface of magnetite and form a stabilizing shell in such a way. The effect of such a shell is remarkably reflected on the curve obtained by us under condition of the maximum content of D₂O in a solvent (Fig. 8) as a specific shoulder at $q = 0.8 \text{ nm}^{-1}$. We note that such a shoulder is almost absent for the MA specimen (Fig. 8).

4. Conclusions

The structural analysis carried out by us with the help of SANS and with the use of a variation of the contrast in aqueous magnetic liquid systems sterically stabilized by short lauric (C12) and myristic (C14) acids has revealed that the liquid systems under study are basically different with respect to the formation of aggregates in them. The experiment executed by us has shown that, in the magnetic liquid system which is stabilized by lauric acid, the polydisperse aggregates of magnetite nanoparticles covered by a double layer of SAS, whose effective thickness is equal to 3.5 nm, are formed. In the magnetic liquid system which is stabilized by myristic acid, the homogeneous and less polydisperse aggregates are formed as a result of the incomplete coverage of magnetite by molecules of SAS. The reason for this fact can be related to a possible creation of micelles of monocarboxyl acids in water, which decreases the number of free molecules of SAS necessary for the complete coverage of the surface of magnetite. As known, the critical concentration for the micelle formation is inversely proportional to the length of a molecule [18], which agrees with the worse stabilization of the magnetic liquid system with longer myristic acid. A larger size and a higher polydispersity of experimentally observed aggregates in the specimen with lauric acid can be explained by a larger size and a higher polydispersity of separate particles which form the aggregate in this case.

1. I.I. Adamenko and L.A. Bulavin, *Physics of Liquids and Liquid Systems* (ASMI, Kyiv, 2006) (in Ukrainian).
2. R.E. Rosensweig, *Ferrohydrodynamics* (Cambridge Univ. Press, Cambridge, 1985)
3. D. Bica, L. Vekas, M.V. Avdeev *et al.*, *J. Mag. Mag. Mater.* **311**, 17 (2007).
4. M.V. Avdeev, V.L. Aksenov, M. Balasoiu *et al.*, *J. Coll. Interface Sci.* **295**, 100 (2006).
5. *Ferrofluids. Magnetically Controllable Fluids and Their Applications*, edited by S. Odenbach, Lecture Notes in Physics, vol. 594 (Springer, Berlin, 2002), p. 233.
6. N.A. Brusnetsov, T.N. Brusnetsova, E.Yu. Filinova *et al.*, *J. Mag. Mag. Mater.* **311**, 176 (2007).
7. C. Sun, J.S.H. Lee, and M. Zhang, *Advanced Drug Delivery Rev.* **60**, 1252 (2008).
8. L. Shen, P.E. Laibinis, and T.A. Hatton, *Langmuir* **15**, 447 (1999).
9. A. Wiedenmann, A. Hoell, and M. Kammel: *J. Mag. Mag. Mater.* **252**, 83 (2002).
10. H.B. Stuhrmann, in *Modern Aspects of Small-Angle Scattering*, edited by H. Brumberger, (Kluwer, Dordrecht, 1995), p. 221.
11. M.V. Avdeev, *J. Appl. Cryst.* **40**, 56 (2007).
12. M.V. Avdeev, D. Bica, L. Vekas *et al.*, *Book of Abstracts, 7th International Conference on the Scientific and Clinical Applications of Magnetic Carriers, Vancouver, May 21-24, 2008* (The University of British Columbia: Vancouver, 2008).
13. H.B. Stuhrmann, N. Burkhardt, G. Dietrich *et al.*, *Nucl. Instr. Meth. A* **356**, 133 (1995).
14. L.A. Bulavin, T.V. Karmazina, V.V. Klepko, and V.I. Sli-senko, *Neutron Spectroscopy of Condensed Media* (Akademperiodyka, Kyiv, 2005) (in Ukrainian).
15. M.V. Avdeev, D. Bica, L. Vékás *et al.*, *J. Mag. Mag. Mater.* **311**, 6 (2007).
16. A.E. Whitten, S. Cai, and J. Trewella, *J. Appl. Cryst.* **41**, 222 (2008).
17. J. Skov Pedersen, *Adv. Coll. Inter. Sci.* **70**, 171 (1997).
18. B. Jounsson, B. Lindman, K. Holmberg, and B. Kronberg, *Surfactants and Polymers in Aqueous Solutions* (Wiley, Chichester, 1998).

Received 12.11.2008

МАЛОКУТОВЕ РОЗСІЯННЯ НЕЙТРОНІВ МАГНІТНИМИ
ВОДНИМИ СИСТЕМАМИ, ЯКІ СТАБІЛІЗОВАНІ
МОНОКАРБОКСИЛЬНИМИ КИСЛОТАМИ

*A.B. Феоктистов, Л.А. Булавін, М.В. Авдеев,
Л. Векаш, В.М. Гарамус, Р. Віллумайт*

Р е з ю м е

З використанням методики варіації контрасту методом мало-
кутового розсіяння неполяризованих теплових нейtronів було

вивчено магнітні рідинні системи, виготовлені на основі води із стеричною стабілізацією. За магнітну наночастинку було використано магнетит, який був вкритий лауриновою або міристиновою кислотами. На основі нового підходу базисних функцій для дослідження полідисперсних суперпарамагнітних систем були отримані дані про структурні особливості магнітних рідин в діапазоні розмірів (1–100) нм. Встановлено, що вид агрегатів магнітних частинок залежить від поверхнево-активної речовини, яку використано для стабілізації магнітної рідинної системи. Показано, що країці стабілізаційні властивості мають зразки зі стабілізацією лауриновою кислотою.